EVALUATION OF THE GAS PRODUCTION POTENTIAL OF CHALLENGING HYDRATE DEPOSITS

George J. Moridis, Matthew T. Reagan, Katie L. Boyle, and Keni Zhang

Lawrence Berkeley National Laboratory
1 Cyclotron Rd.
Berkeley, CA 94720, USA
e-mail: GJMoridis@lbl.gov

ABSTRACT

We use the TOUGH+HYDRATE code to assess the production potential of challenging hydrate deposits, i.e., deposits that are characterized by any combination of the following factors: absence of confining boundaries, high thermodynamic stability, low temperatures, low formation permeability. Using high-resolution grids, we show that a new horizontal well design using thermal stimulation coupled with mild depressurization yields production rates that appear modest and insufficient for commercially viable production levels. The use of parallel horizontal wells (with the lower one providing thermal stimulation through heat addition, direct injection or circulation of warm water, and the upper one producing under a mild depressurization regime) offers tantalizing possibilities, and has the potential of allowing commercial production from a very large number of hydrate deposits that are not currently considered as production candidates if the problem of the corresponding large water production can be solved.

INTRODUCTION

Gas hydrates are solid crystalline compounds in which gas molecules are lodged within a clathrate crystal lattice (Sloan and Koh, 2008). Vast amounts of CH_4 stored in hydrates in geologic media in the permafrost and in the oceans. The current study is part of a larger effort to determine the technical feasibility of gas production from a wide range of hydrate deposits in geologic media.

Recent studies have determined the conditions, methods and characteristics that enhance production from such deposits. The most important features (Moridis et al., 2008) include (a) high temperatures and pressures (the deepest, warmest deposits are the most desirable), (b) thermodynamic proximity to the H-V-Lw equilibrium conditions (Figure 1), (b) the use of depressurization, because pure thermal stimulation appears to be very slow and ineffective (Moridis and Reagan, 2007a;b), (c) the presence of impermeable boundaries and, in the case of Class 2 systems, thin water zones, and (d) high intrinsic permeabilities of the hydrate-bearing sediments. If these conditions are met, hydrate deposits can yield methane at high rates (well in excess of 10 MMSCFD) for long periods using conventional production technology (Moridis and Reagan, 2007a;b).

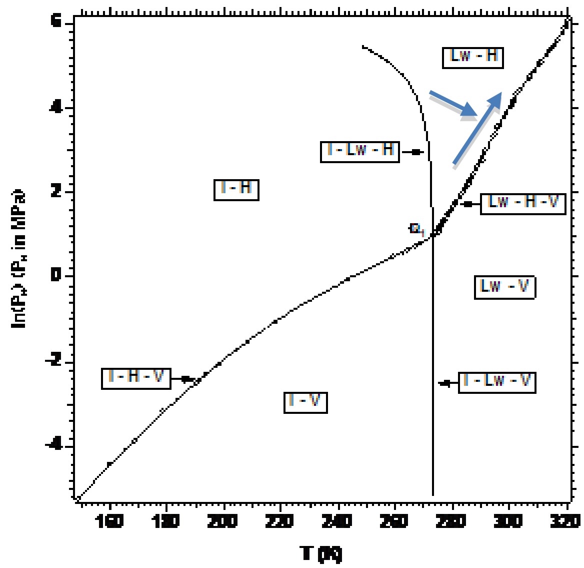

Figure 1. Pressure-temperature equilibrium relationship in the phase diagram of the water–CH_4–hydrate system (Moridis, 2003). The two arrows show the direction of increasing thermodynamic desirability of a deposit as a production target.

Challenging Hydrates

In this study we address the issue of gas production from "challenging" hydrates (CG), i.e. those that do not meet the desirability criteria discussed earlier. Such CG include: (a) absence of impermeable boundaries (CG-B), (b) low initial temperatures, and, consequently, pressures (CG-T), (c) increased stability, as indicated from their thermodynamic distance from the hydrate equilibrium conditions (CG-S), (d) extremely low effective permeability k_{eff}, caused either by very high hydrate saturations S_H (CG-H), and/or by occurrence in fine-textured sediments, low-k media such as silts and clays (CG-k). An additional type of CG includes hydrate chimneys (CG-C), i.e., marine hydrates that occur at high S_H in near-vertical cylindrical structures that are associated with past CH_4 plumes, often extend to the ocean floor, and usually have limited diameters (usually < 30 m) and no confining boundaries.

Dissociation is orders of magnitude more effective than thermal stimulation as a dissociation method for gas production (Moridis and Reagan, 2007b). However, a common feature of all cases of CG is that depressurization cannot be effectively applied because of (1) the absence of low-k boundaries and high water production (CG-B, CG-C), (2) the very low k_{eff}, (CG-H, CG-k, CG-C), (3) the impracticality of effecting the very large pressure drops needed to cause dissociation of very stable hydrates (CG-S), or (4) low sensible heat to sustainably fuel depressurization-induced dissociation (CG-T). The high cost and progressively diminishing effectiveness of chemical inhibitors precludes their intensive use for gas production from CG, and pure thermal stimulation has been shown to be ineffective (Moridis and Reagan, 2007b). Conjunctive use of thermal stimulation with depressurization appears to be a plausible method for gas production from CGs.

Objectives

In this study we investigate by means of numerical simulation the production potential of some types of CGs. We focus on CG-B, but we also investigate production from CG-T and CG-k through sensitivity analysis. Additionally, we investigate the effectiveness of two different well designs. We evaluate production according to two criteria: the *absolute* criterion of gas production, and the *relative* criterion of the gas-to-water ratio.

GEOLOGIC AND NUMERICAL MODEL

The geologic system in this study is based the Tigershark area, located in the Alaminos Canyon Block 818 of the Gulf of Mexico. Log data from a specially designed exploration well in about 2750 m (9000 ft) of water at the site indicated the presence of an 18.25-m (60-ft) thick sandy hydrate-bearing layer (HBL) corresponding to a drilling depth. The HBL has a porosity ϕ of about 0.30 and Darcy-range intrinsic permeability k. Initial estimates of gas hydrate saturation S_H derived from analyses of the resistivity and p-wave velocity data indicate a range from 0.6 to over 0.8. Preliminary calculations indicated that the base of the gas hydrate stability zone at this location occurs at or slightly below the base of the HBL. Because of uncertainty about its boundaries, Moridis and Reagan (2007a;b) investigated production from the Tigershark deposit both as a Class 2 deposit (HBL overlying a mobile water zone) and a Classs 3 system (HBL bounded by impermeable strata, with no underlying zone of mobile fluids). They showed that the presence of near-impermeable boundaries can yield very high rates (as high as 17 MMSCFD in Class 2, up to 15 MMSCFD in Class 3). However, sensitivity analysis (Reagan et al., 2008; Boswell et al. 2009) indicated that lack of impermeable boundaries can dramatically reduce gas production (Figure 2), while yielding very large amounts of water. Here we investigate the production potential of the Tigershark formation under the hypothesis of a worst-case scenario, i.e., absence of impermeable boundaries, and contact of the hydrate layer with practically infinite aquifers.

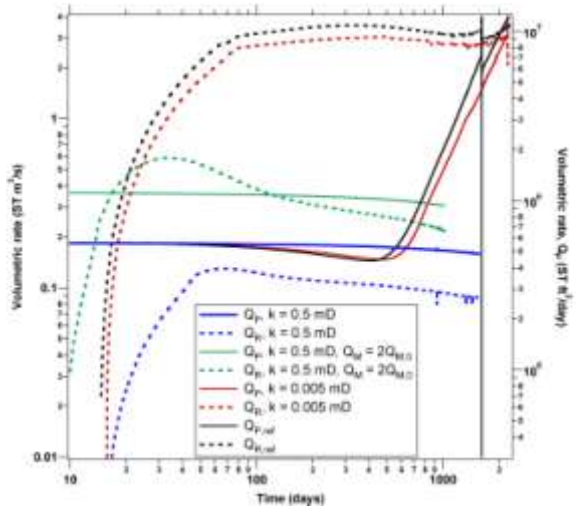

Figure 2. Effect of boundary permeability on gas production from a Tigershark Class 3 deposit (Reagan et al., 2008).

This study involves horizontal wells because of their significant advantages over vertical wells in production from Class 2 and Class 3 deposits (Moridis and Reagan, 2008). We investigated two different horizontal well designs. The single-well of the first design (Figure 3) provides heat to the hydrate-bearing sediment (HBS) by means of hot water that circulates inside the wellbore without coming in contact with the hydrate. The resulting higher T is expected to promote hydrate dissociation and gas production through the configuration of Figure 3 that operates at a pressure P_w that is slightly lower than the initial pressure P_0. By avoiding direct injection of the warm water into the HBS we do not create adverse relative permeability conditions for the flow evolving gas, and the mild depressurization limits the water production. The second design is akin to that used in heavy oil production, and involves two parallel horizontal wells. Heat (through circulation of warm water, electrical or microwave heating, or direct water injection into the HBL) is added to the HBL through the lower well, while the upper well (positioned on the same vertical plane) is the gas collection well operates at a mild depressurization regime. In both well designs, the source of the warm water is assumed to be a deeper warmer reservoir.

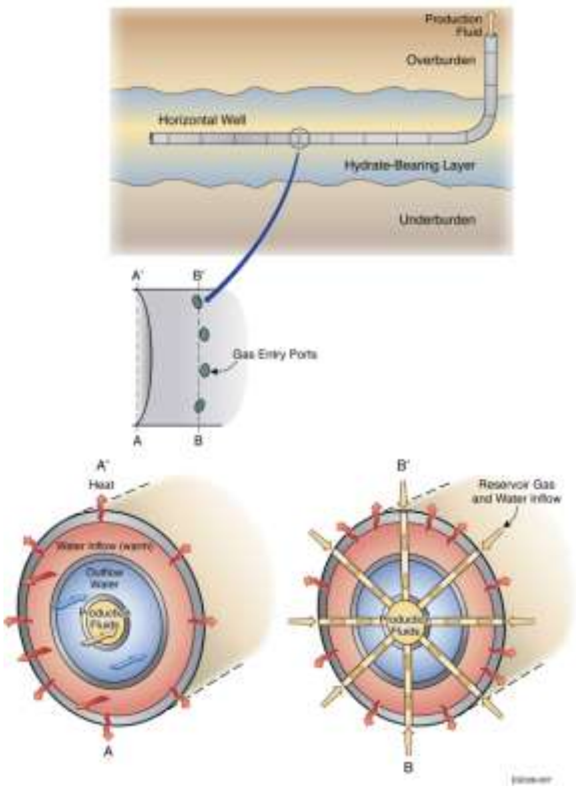

Figure 3. The new well design for concurrent heat addition and gas production.

We conducted the simulations using the TOUGH+HYDRATE code (Moridis et al., 2008). This code can model the non-isothermal hydration reaction, phase behavior, and flow of fluids and heat under conditions typical of natural CH_4-hydrate deposits in complex geologic media. It includes both an equilibrium and a kinetic model of hydrate formation and dissociation. The model accounts for heat and up to four mass components (i.e., water, CH_4, hydrate, and water-soluble inhibitors such as salts or alcohols) that are partitioned among four possible phases: gas, aqueous liquid, ice, and hydrate. A total of 15 states (phase combinations) can be described by the code, which can handle any combination of hydrate dissociation mechanisms.

We used 2-D grids because of symmetry. The unstructured hybrid grids used in the simulations are shown in Figures 4 and 5, and comprised 47,000 and 27,000 elements, respectively (resulting in 288,000 and 108,000 coupled equations). The system properties and initial conditions are as described by Moridis and Reagan (2007a;b) and shown in Table 1. Both grids had open top and bottom boundaries, i.e., the HBL was connected with the permeable overburden and underburden, allowing fluid and heat flow through the boundaries. The x = 40 m boundary was closed, indicating a well spacing of 80 m.

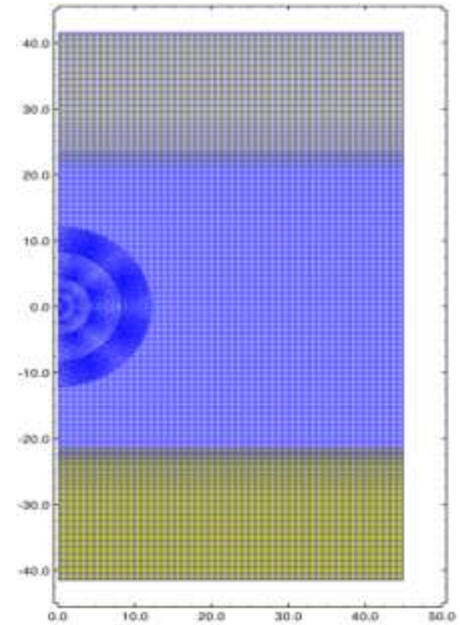

Figure 4. Grid used in the study of the performance of the new well design of Figure 3.

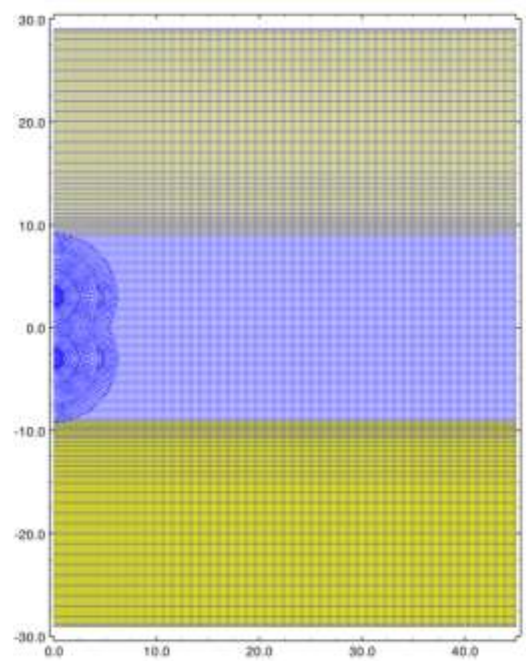

Figure 5. Grid used in the study of the performance of the two parallel horizontal well system.

THE SINGLE WELL DESIGN

In the evaluation of the single-well design, the reference case involved the sandy HBS (k = 7.5x10^{-13} m^2) described in the Moridis and Reagan (2007a;b) study, and the temperature of the circulating hot water was T_w=90 ^{o}C. Sensitivity analysis was investigated through the following additional cases: (a) T_w=120 ^{o}C, (b) a silty medium with k = 7.5x10^{-14}

m^2, (c) a clayey medium with k = 7.5x10^{-15} m^2, and (d) lower (by 10 °C) initial T, i.e., a more stable hydrate at the prevailing P.

Table 1. Physical properties and simulation parameters for the 2-D hydrate-bearing system.

Parameter	Value
Hydrate zone thickness	18.25 m
Initial pressure P_B (at base of HBL)	3.3x10^7 Pa
Initial temperature T_B (at base of HBL)	294.15 K (21 °C)
Gas composition	100% CH_4
Initial saturations in the HBL	$S_H = 0.7$, $S_A = 0.3$
Water salinity (mass fraction)	0.03
Initial saturations in the HBL	$S_H = 0.7$, $S_A = 0.3$
Intrinsic permeability k_r=k_z (HBS and boundaries)	7.5x10^{-13} m^2 (= 0.75 D)
Grain density r_R (all formations)	2750 kg/m^3
Dry thermal conductivity k_{QRD} (all formations)	0.5 W/m/K
Wet thermal conductivity k_{QRW} (all formations)	3.1 W/m/K
Composite thermal conductivity model (Moridis et al., 2005)	$k_{QC} = k_{QRD} + (S_A^{1/2} + S_H^{1/2})(k_{QRW} - k_{QRD}) + f S_I k_{QI}$
Capillary pressure model (vanGenuchten, 1980)	$P_{cap} = -P_0 \left[(S^*)^{-1/\lambda} - 1 \right]^{\lambda}$ $S^* = \frac{(S_A - S_{irA})}{(S_{mxA} - S_{irA})}$
S_{irA}	1
l	0.45
P_0	10^5 Pa
Relative permeability Model (Moridis et al., 2008)	$k_{rA} = (S_A{*})^n$ $k_{rG} = (S_G{*})^n$ $S_A{*}=(S_A-S_{irA})/(1-S_{irA})$ $S_G{*}=(S_G-S_{irG})/(1-S_{irA})$ OPM model
n (from Moridis and Reagan, 2007a;b)	3.572
S_{irG}	0.02

<u>The Reference Case and the T_w = 120 °C Case</u>

Figure 6 to 9 show respectively the evolutions of the following variables over time: P, T, S_H and S_G. The very low pressure drop ΔP (Figure 6) is evident in that it creates an anomaly fully confined in a limited zone around the well. This is caused by the low effective permeability k_{eff} of the HBL in the area surrounding the dissociated zone (Figure 8). As expected, the temperature disturbance does not propagate far from the well because of the limited efficiency of conduction as the main heat transfer mechanism, and the rate of its propagation declines significantly over time as the volume around the well increases as a function of r^2. A direct consequence of the limited advance of the temperature front is the limited extent of the dissociated region (Figure 8).

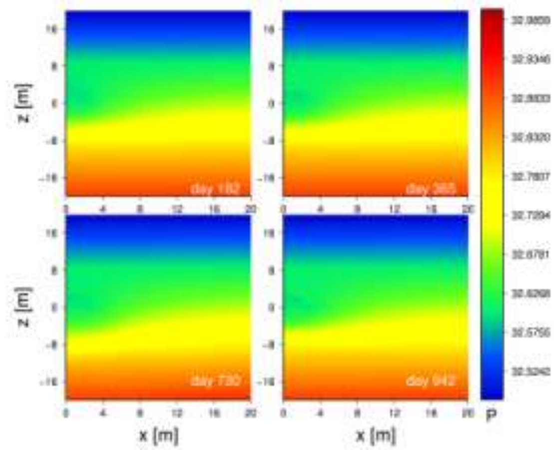

Figure 6. Evolution of pressure P over time during production from the single well of Figure 3.

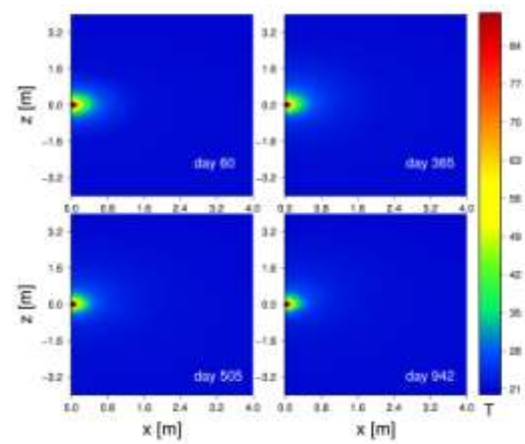

Figure 7. Evolution of temperature T during production from the single well of Figure 3.

Of particular interest is the high-S_H region immediately ahead of the dissociation front (Figure 8). This occurs because the edge of this front is the locus of local maximum of P in the system, with fluids moving both away and toward the well. Gas moving deeper into the hydrate body (away from the well) encounters conditions that are conducive to secondary hydrate formation that result in S_H higher than the initial one. The S_G distribution in Figure 10 indicates that practically all the dissociated gas that has not been produced is trapped within the hydrate-free cylindrical zone defined by the dissociation front. Because of buoyancy, gas accumulates at the top of the cylindrical dissociated zone, while the water released from dissociation drains and accumulates at the bottom of the cylindrical hydrate-free zone.

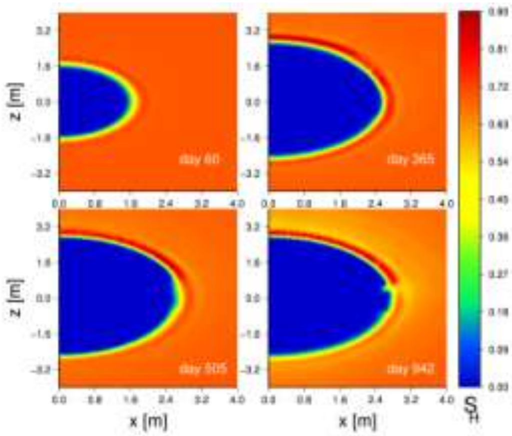

Figure 8. Evolution of hydrate saturation S_H during production from the single well of Figure 3.

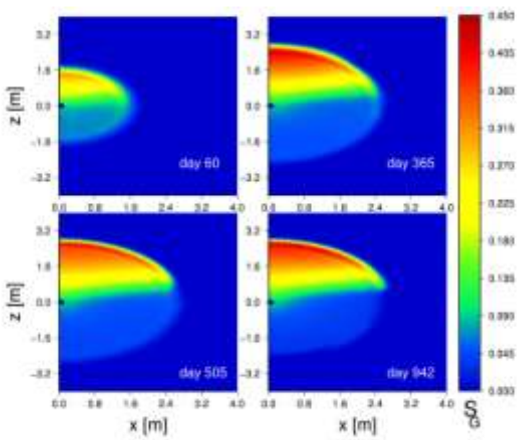

Figure 9. Evolution of gas saturation S_G during production from the single well of Figure 3.

Figure 10 shows the volumetric rates (per linear m of the horizontal well) of CH_4 (a) release Q_R, (b) production in the gas phase Q_{PG}, and (c) total gas production Q_{PT}, i.e., both in the gas and aqueous phase for the T_w= 90 °C and 120 °C cases. Note that Q_{PT} exceeds Q_R, and that the majority of the produced gas comes from CH_4 dissolved in the water rather than from the free gas phase, and that. The production rates appear to be quite low, even if we assume that all the dissolved CH_4 (a very significant fraction of Q_{PT}) is recovered. Additionally, the higher T_w appears to have a limited effect on gas production, increasing Q_{PT} only slightly over the 90 °C case. The corresponding water production rates Q_w and gas-to-water ratios R_{GW} = V_P/M_w in Figure 12 show the larger T_w has slight (if any) practical effect, that water production is manageable and that the R_{GW} is not prohibitively low. However, for a 1000 m well, long-term Q_{PT} < 7,000 ST m^3 (245 MSCFD), and about 40 times lower than the rule-of-thumb for commercially viable production rates from offshore gas wells.

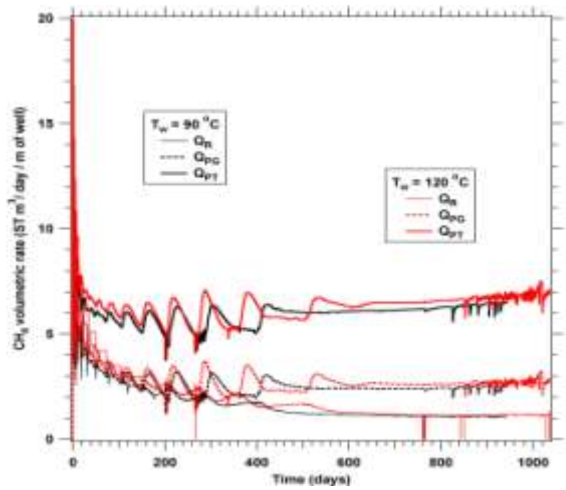

Figure 10. Evolution Q_R, Q_{PG} and Q_{PT} during production from the single well of Figure 3.

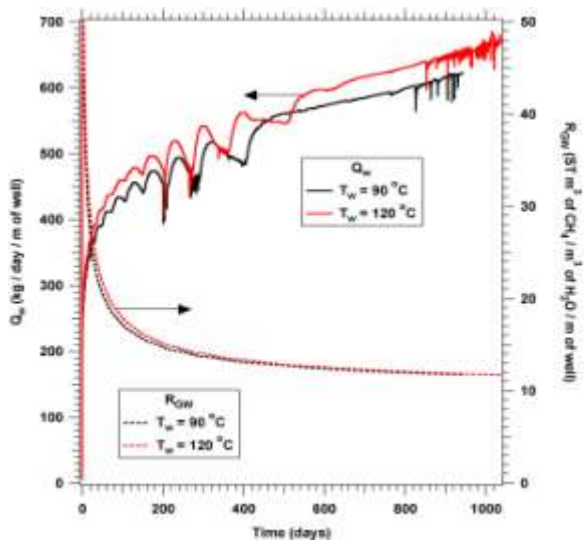

Figure 11. Evolution Q_W and R_{GW} during production from the single well of Figure 3

Effect of Finer Texture-Media (Lower k)

Figure 12 shows Q_R, Q_{PG}, and Q_{PT} in (a) the reference case of a sandy HBL, (b) the case of a silt, (c) a clay with a low well pressure drop ΔP_w = 1 atm (Case Clay-LP), and (d) a clay case of a higher ΔP_w = 5 atm (case Clay-HP). The decreasing permeability k and increasing capillary pressure P_{cap} of a progressively finer texture (moving from a sand to a clay) leads to an increasing Q_R, but a decreasing Q_{PT}. Thus, Q_{PT} from the sandy system (already quite low) is the highest of all cases. Additionally, the contribution of production in the gas phase Q_{PG} increases with a decreasing permeability. As expected, the higher ΔP_w leads to higher Q_R, Q_{PG}, Q_{PT}, Q_W, and R_{GW}, but Q_{PT} is still lower than that for the sandy HBS.

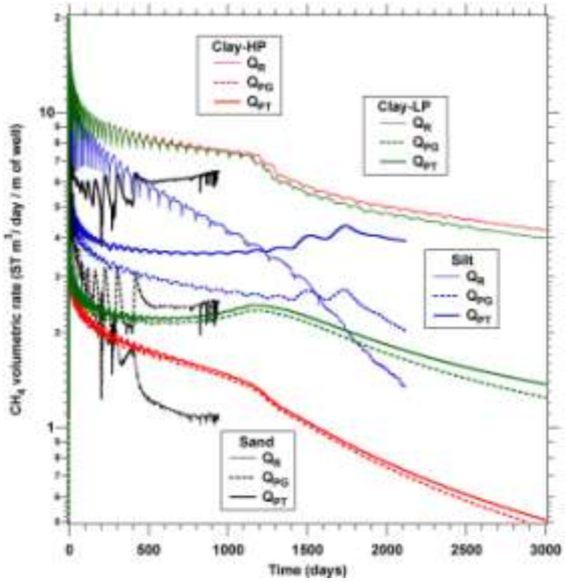

Figure 12. Effect of HBS texture on Q_R, Q_{PG} and Q_{PT} during production from the single well.

The corresponding Q_w and R_{GW} in Figure 13 show that water production increases with the fineness (decreasing k and increasing P_{cap}) of the HBS texture, but R_{GW} exhibits the opposite pattern. The high R_{GW} in silt and clay systems (relative criterion) cannot compensate for the low production (absolute criterion).

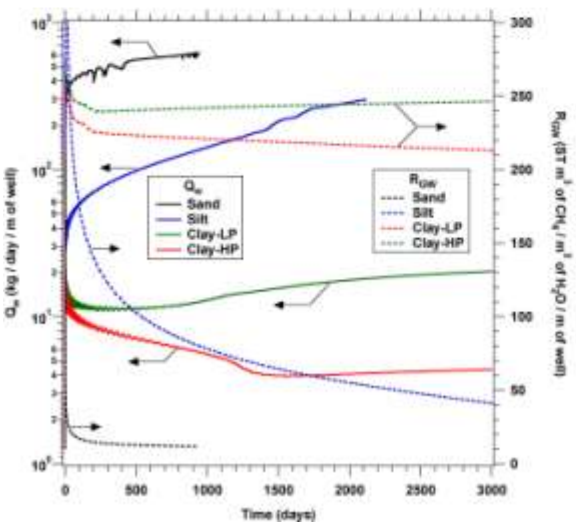

Figure 13. Effect of HBS texture on Q_W and R_{GW} during production from the single well.

Effect of Temperature

Figure 14 shows Q_R, Q_{PG}, and Q_{PT} in a silty HBL with (a) the reference initial T_0 = 21 °C, and (b) in a colder system with T_0 = 11 °C at the same pressure, and indicates that lower T_0 results in significantly lower gas production. Additionally, Figure 15 indicates that the lower Q_{PT} of the colder case is further burdened by a lower R_{GW} despite a decreasing Q_w. This was expected because the k_{eff} and the corresponding Q_w remain low during the longer time it takes for the colder (and thermodynamically more stable) HBL to reach the dissociation temperature at the prevailing pressure.

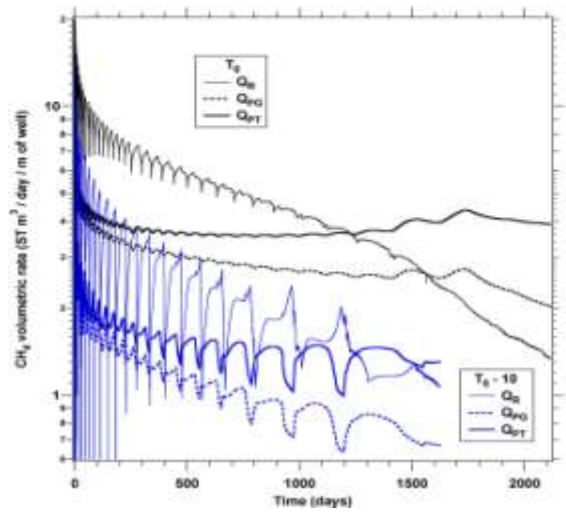

Figure 14. Effect of temperature on Q_R, Q_{PG} and Q_{PT} during production from the single well.

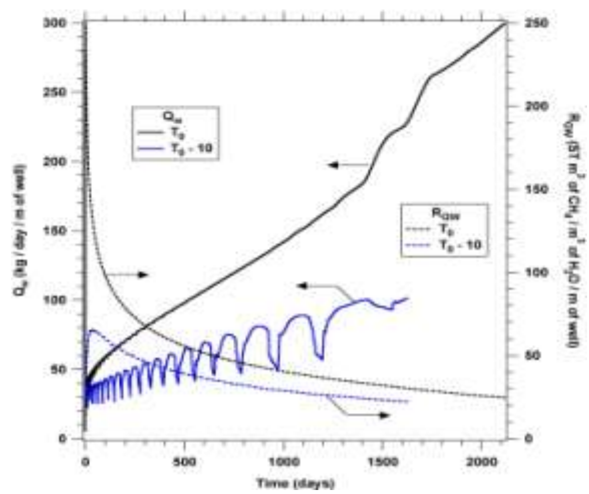

Figure 15. Effect of temperature on Q_W and R_{GW} during production from the single well.

THE TWO-WELL DESIGN

We study the following cases, all involving sandy systems: (a) Case A, with hot water (T_w = 90 °C) circulating in the lower well (LW) without entering the HBL, and the upper well (UL) operating at a ΔP_w = 1 atm, (b) Case B1, with heat added to the HBL at a rate of 1000 W/m, and a ΔP_w = 1 atm at the UW, (c) Case B2, diferring from B1 in that ΔP_w = 0.2 P_0, (d) Case C1, with warm water (T_{iw} = 60 °C) injected into the HBL through the LW at a rate of Q_{iw} = 5x10^{-3} kg/s/m of the well, and ΔP_w = 1 atm at the UW, (e)

Case C2, differing from C1 in that $\Delta P_w = 0.1\ P_0$, and (f) Case C3, differing from C1 in that $\Delta P_w = 0.2\ P_0$.

Cases A, B1 and B2

Figure 16 shows that in Cases A and B1, no CH_4 is ever produced in the gas phase ($Q_{PG} = 0$), i.e., all the produced gas originated from CH_4 dissolved in the aqueous phase. The low Q_{PT} ceases completely after only about 52 days. Q_R continues past that time because of the continuous heat addition, but this does not lead to continuous gas production because the released gas remains trapped in a dissociated, hydrate-free cylindrical zone that is surrounded by hydrate at very high saturations that exceed the initial S_H (Figure 17). This is caused by gas from dissociation moving into the HBL and creating secondary hydrates that reach levels resulting in a reduction of k_{eff} to practically zero. Note that secondary hydrates are also formed around the producing UW. In Figure 17, the gas and water accumulation at the top and the bottom, respectively, of the isolated cylindrical zone are evident.

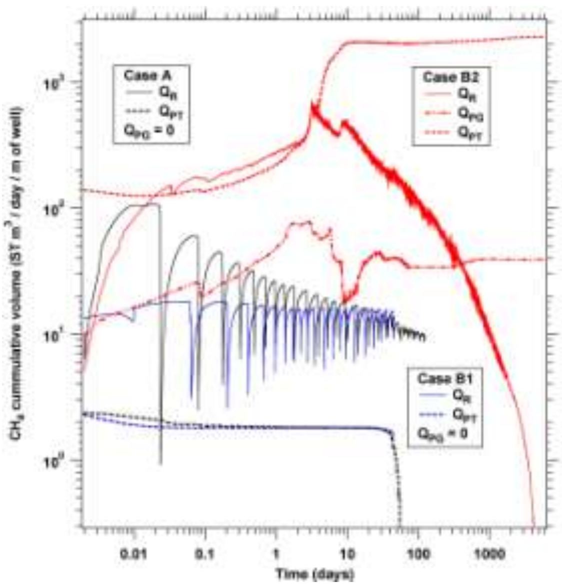

Figure 16. Evolution of Q_R, Q_{PG} and Q_{PT} during production from the two-well system (Cases A, B1, and B2).

Figure 18 confirms the creation of the isolated zone by showing Q_W declining to zero at the same time that Q_{PT} tends to zero. This was expected because no free gas is ever produced, and flow of the aqueous phase is necessary to obtain the dissolved CH_4 (the only gas source in these cases).

Case B2 appears very different. Figure 16 indicates order of magnitude higher Q_R and Q_{PT} in addition to a large Q_{PG}, all of which are attributable to the stronger depressurization (as the thermal regime remains the same). Thus, the thermal stimulation in the LW serves only to develop an initial Q_R reaches a maximum after about 3 days, and then declines continuously until it is reduced to zero after about 4,000 days when the hydrate is exhausted. Q_{PG} is practically constant after about 60 days, while Q_{PT} exhibits a jump at 3 days (corresponding roughly to the depressurization front reaching the upper boundary of the HBL), and remains practically constant after 10 days.

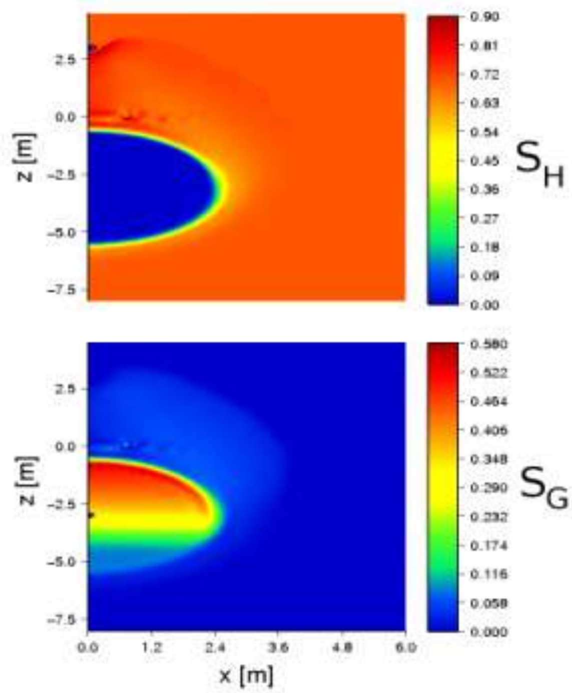

Figure 17. Distribution of S_H and S_G during production from the two-well system at t = 60 days (Case A).

This is confirmed by Figure 18, which shows a step increase in Q_w at t = 3 days, and a constant Q_w after about 10 days that corresponds to a significant reduction in R_{GW}. Thus, Q_{PT} for a 1000 m well system reaches a long-term near-constant level of 2.2×10^6 ST m^3/day (76 MMSCFD), this is hampered by a large water production.

The reason for this promising Q_{PT} performance is the effectiveness of depressurization as a dissociation method, as demonstrated by the S_H distribution over time in Figure 19. The corresponding P and T distributions in Figures 20 and 21, respectively, show the establishment of a steady state pressure regime (because of the permeable boundaries) and the negligible effect of the warm water injection, which appears to be completely overwhelmed by the effects of depressurization (evident by the changes in the T

distribution over time in the vicinity of, and within, the hydrate body).

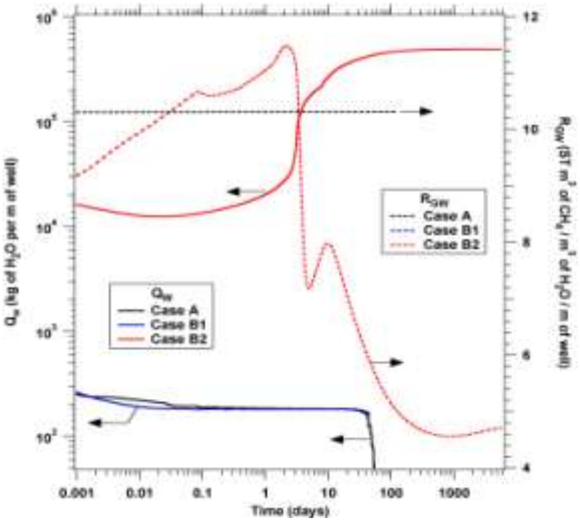

Figure 18. Evolution of Q_R, Q_{PG} and Q_{PT} during production from the two-well system (Cases A, B1, and B2).

Cases C1, C2 and C3

The Q_R, Q_{PG}, and Q_{PT} in Figure 22 indicate that, in Case C1, warm water injection appears to have a worse overall effect than the heat addition methods in Cases A and B1. As in these cases, no CH_4 is ever produced in the gas phase (Q_{PG} = 0), but the low Q_{PT} ceases completely after 21.6 days because of significant secondary hydrate creation around the UW and around the hydrate-free cylindrical zone of complete dissociation (Figure 23), which brings k_{eff} down to zero levels at these locations. The Q_R curve is entirely analogous to that of Case A in Figure 16, as are the S_H and S_G distributions in Figure 20.

The Q_R, Q_{PG}, and Q_{PT} of Case C3 in Figure 22 are indistinguishable from those in Case B2, indicating (a) large production potential for this approach, and (b) that the heat addition method plays a minimal role in the pattern of the system response (and possibly only to create an initial high-k_{eff} zone to allow further dissociation by means of depressurization). Figure 24 shows the similarity of the Q_W and R_{GW} between Cases A, B1 and C1, in addition to the practical coincidence of the system behavior in Cases B2 and C3.

Case C2 appears quite different. While its Q_R, Q_{PG}, and Q_{PT} curves in Figure 19 initially appear to track those for Case C2 (albeit at a lower level because of the lower ΔP_w), Q_R and Q_{PG} are reduced to zero levels after 34 and 18 days, respectively, because ΔP_w is insufficient to prevent the formation of an isolated hydrate-free zone surrounded by high S_H. Water production continues past this point because the flow to the UW is not blocked (Figure 24), but Q_{PT} is reduced because dissolved gas is the only source of CH_4.

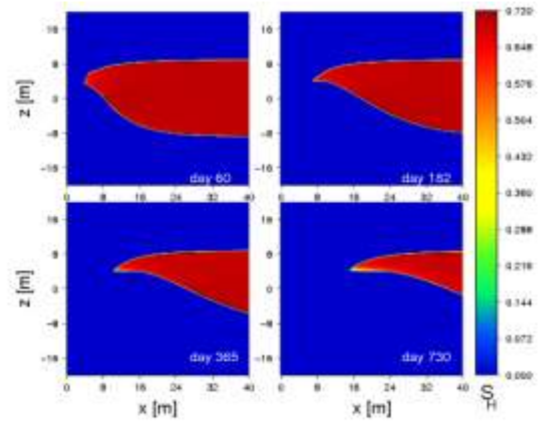

Figure 19. Evolution of hydrate saturation S_H distribution during production in Case C3.

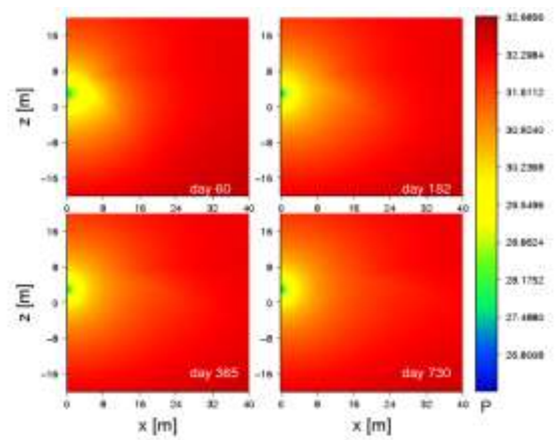

Figure 20. Evolution of pressure P distribution during production in Case C3.

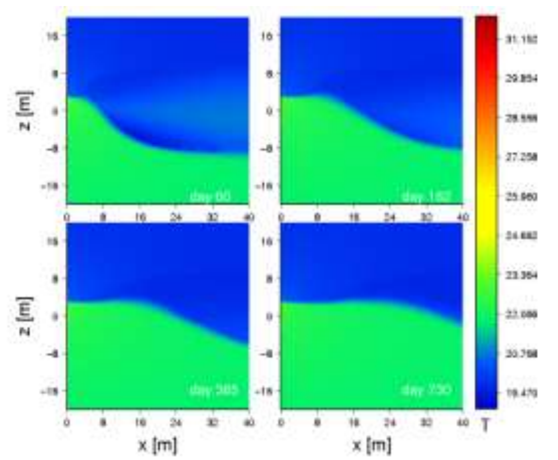

Figure 21. Evolution of reservoir temperature T distribution during production in Case C3.

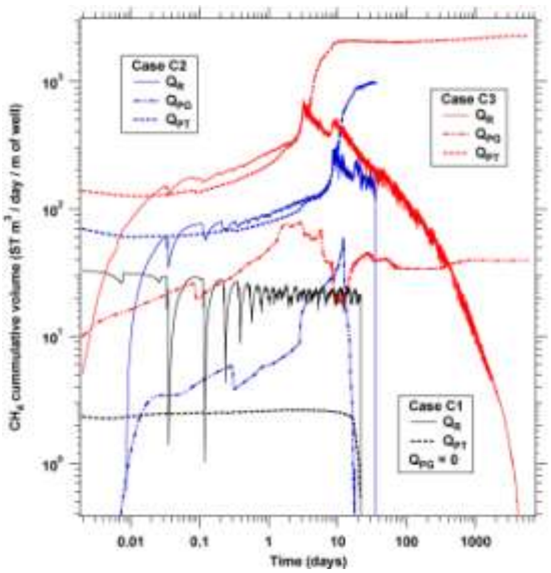

Figure 22. Evolution of Q_R, Q_{PG} and Q_{PT} during production from the two-well system (Cases C1, C2, and C3).

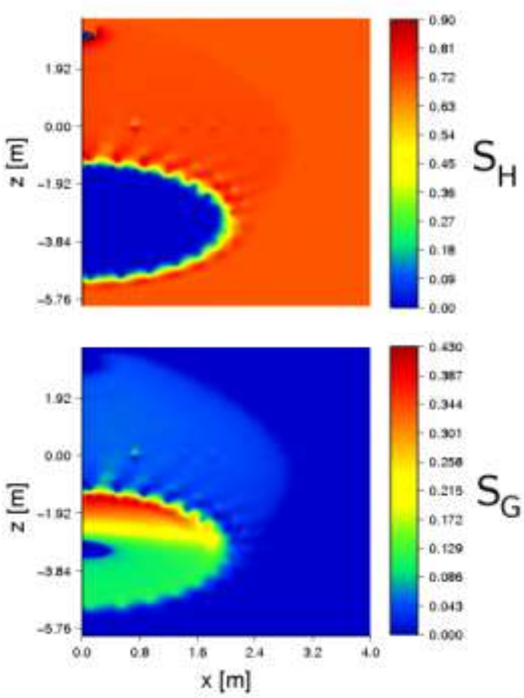

Figure 23. Distribution of S_H and S_G during production from the two-well system at t = 21.6 days (Case C1).

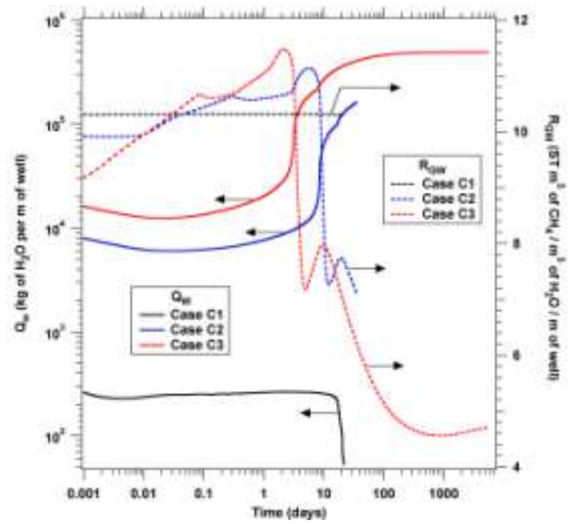

Figure 24. Evolution of Q_R, Q_{PG} and Q_{PT} during production from the two-well system (Cases C1, C2 and C3).

CONCLUSIONS

We reach the following conclusions from this study:

- The use of the new, single-well design involving concurrent HBL heating and production from different segments along the same wellbore does not appear a promising solution to the problem of production from challenging hydrates because it results in very low gas production rates and unfavorable gas-to-water ratios.
- Using the new, single-well design, production increases with the coarseness of the HBS (i.e., with an increasing k and P_{cap}, thus favoring sandy over silty and clayey HBS) and with the initial temperature of the deposit. Using a lower well (bottomhole) pressure P_w increases gas production, but it also increases the undesirable water production.
- If the P_w of the UW is maintained at levels very close to P_0, the two parallel horizontal well system appears to be very ineffective, resulting in very short production times before flow to the UW is blocked by secondary hydrate that brings the k_{eff} to zero levels.
- If P_w = 0.8 P_0 in the UW, then depressurization is by far the dominant process and effective dissociation occurs, resulting in high gas production rates (up to 76 MMSCFD). However, the gas production is accompanied by a large water production.

ACKNOWLEDGMENT

This work was supported by the Assistant Secretary for Fossil Energy, Office of Natural Gas and Petroleum Technology, through the National Energy Technology Laboratory, under the U.S. Department of Energy, Contract No. DE-AC02-05CH11231. The authors are indebted to John Apps and Dan Hawkes for their careful review.

REFERENCES

Boswell, R., D. Shelander, M. Lee, T. Latham, T. Collett, G. Guerin, G. Moridis, M. Reagan and D. Goldberg, Occurrence of gas hydrate in Oligocene Frio sand: Alaminos Canyon Block 818: Northern Gulf of Mexico, J. Mar. Pet. Geo., *26*, 8, 1499-1512, 2009.

Moridis, G.J., Numerical Studies of Gas Production from Methane Hydrates, *SPE Journal*, *32*(8), 2003.

Moridis, G.J., Seol, Y., and T. Kneafsey, Studies of reaction kinetics of methane hydrate dissociation in porous media (Paper 1004), *Proceedings of the 5th International Conference on Gas Hydrates*, Trondheim, Norway, 12-16 June 2005.

Moridis, G.J., and M.T. Reagan, Strategies for Gas Production From Oceanic Class 3 Hydrate Accumulations, OTC-18865, *Proceedings of the 2007 Offshore Technology Conference*, Houston, Texas, 30 April – 3 May, 2007a

Moridis, G.J., and M.T. Reagan, Gas Production From Oceanic Class 2 Hydrate Accumulations, OTC 18866, *Proceedings of the 2007 Offshore Technology Conference*, Houston, Texas, U.S.A., 30 April–3 May 2007.

Moridis, G.J., Kowalsky, M.B., and K. Pruess, *TOUGH+HYDRATE v1.0 User's Manual: A Code for the Simulation of System Behavior in Hydrate-Bearing Geologic Media,* Report LBNL-0149E, Lawrence Berkeley National Laboratory, Berkeley, CA.

Reagan, M.T., Moridis, G.J., and Zhang, K., Sensitivity Analysis of Gas Production from Class 2 and Class 3 Hydrate Deposits, OTC 19554, *Proceedings of the 2008 Offshore Technology Conference*, Houston, Texas, USA, 5-8 May 2008.

Sloan, E.D. and C. Koh, *Clathrate Hydrates of Natural Gases*, CRC Press, New York, NY, 2008.

Van Genuchten, M.T., A closed-form equation for predicting the hydraulic conductivity of unsaturated soils, *Soil Sci. Soc.*, *44*, 892-898, 1980.